

Effective Illumination Control for an Active Spectral Imaging System

Takahiko Horiuchi, Hirokazu Kakinuma and Shoji Tominaga
Graduate School of Advanced Integration Science, Chiba University, Chiba, Japan

Abstract

A high-speed spectral imaging system using an active spectral illumination has a big potential in the spectral color imaging field. However, it has been difficult to produce an accurate target illuminant because the basis illuminants are not ideal narrow-band spectra. Therefore, we need a mechanism of appropriate adjustments for emitting the desired illuminants from the light source. This paper proposes a control method for producing an arbitrary target illuminant precisely from the active spectral light source by combining the light source with a measurement device. We construct two types of illuminant control systems. The first system uses a high-speed monochrome camera as the measurement device. In this system, we determine the desired sequence of the camera outputs in advance. Then we adjust the light source system for generating the target camera outputs by a feedback control. The second system uses a spectroradiometer as the measurement device. In this system, the target is the spectral-power distribution determined by multiplying the surface-spectral reflectance to the illuminant. The system adjusts the light source for producing the optimum illuminant with the target spectrum by the feedback control. We consider two applications of the illuminant control system to (1) accurate generation of a target illuminant and (2) estimation of surface-spectral reflectances without knowing the camera spectral sensitivity function.

Introduction

An active spectral illumination has a big potential in the spectral color imaging field, and a few interesting approaches were proposed for the purpose of color classification [1] and surface reflectance recovering [2]. However, the coexisting of accuracy and speed was difficult for producing a desired illuminant. A high-speed spectral imaging system using an active spectral illumination was proposed by the authors [3],[4] using a programmable light source. So far we showed effective applications using the imaging system such as a quick estimation of surface-spectral reflectances, a new method for colorimetry, and a visual evaluation system under arbitrary illuminants [3]. They also showed the possibility of real time colorimetry and a good performance for static objects and moving objects [4].

It is essential to produce a target illuminant with a desired spectrum using the active spectral light source in practical applications. For example, we have to emit an inverse sensor-spectral sensitivity function to a target object for estimating the surface-spectral reflectance [3], and emit the XYZ color-matching functions to an object for estimating the tristimulus values [4]. However, the control of producing the desired illuminant spectra was not so easy because (1) the basis spectral functions of the light source do not have the ideal property of narrow-band, and (2) the intensity variation is not linear. Moreover, the intensity of illuminant spectrum projected on an object surface depends on the distance from the light source and

the illumination angle. In the previous papers, the intensities of the basis spectral functions were controlled for emitting the target spectrum.

The present paper proposes an automatic control system for effectively producing arbitrary illuminants from the active spectral light source. The light source used in this study is a programmable spectral source which is capable of emitting illuminant spectra in high speed [5]. We consider two types of feedback control systems by combining the high-speed spectral light source and two measurement devices as shown in Fig. 1.

The first system is an *illuminant-camera system* which uses a monochrome camera as the measurement device (see Fig. 1(a)). In this system, we determine the desired sequence of the camera outputs in advance. Then we adjust the light source system for generating the target camera outputs by a feedback control. The target is the camera outputs multiplying the surface-spectral reflectance and the sensor-spectral sensitivity to the illuminant. This feedback control system makes it possible to produce an illuminant with the inverse function spectrum of the camera-spectral sensitivity without measuring the actual camera-spectral sensitivity. As a result, we can estimate surface-spectral reflectances of arbitrary objects at each pixel point on the camera.

The second system is a *spectroradiometer-camera system* which uses a spectroradiometer directly as the measurement device (see Fig. 1(b)). In this system, the target is the spectral-power distribution determined by multiplying the surface-spectral reflectance to the illuminant. As a result, we can directly produce the desired illuminant spectrum by a feedback control. The performance of producing standard illuminants automatically can be examined in a very short time.

In the following, Section 2 describes the structure of an imaging system using an active spectral light source and a basic control of illuminant emission. Section 3 describes the proposed feedback control systems and the algorithms. Section 4 shows two applications of the surface-spectral reflectance estimation and the arbitrary illuminant production.

Imaging System using Active Spectral Light Source

We briefly describe the present imaging system using active spectral light source. The system consists of a high speed monochrome camera (Epix SV642M), a programmable light source (Optronic Laboratories OL490) [5], a Liquid light guide, and personal computers for controlling the camera and the light source.

The programmable light source is composed of a xenon lamp source, a grating, a digital micromirror device (DMD) chip, and a liquid light guide. In this system, a light beam of xenon is separated by the grating into its constituent wavelengths. The wavelength and intensity information is controlled using the two-dimensional DMD chip, where one axis corresponds to the wavelength distribution of the spectrum, and the other axis to the intensity distribution [5]-[9]. The micromirrors on the DMD

have two ON-OFF bistable states, which control the incident light. That is, the output intensity levels are controlled by the number of DLP mirrors toggled in the ON state. We use the chip of 1024x768 pixels, where the former number influences the wavelength resolution in the range of 380-780nm and the latter number determines the intensity quantization level. As an advantage of the DMD-based programmable light source, it can switch the output light spectrum much faster than a light source based on a liquid-crystal display [10], enabling real-time spectral image acquisition with a high-speed camera.

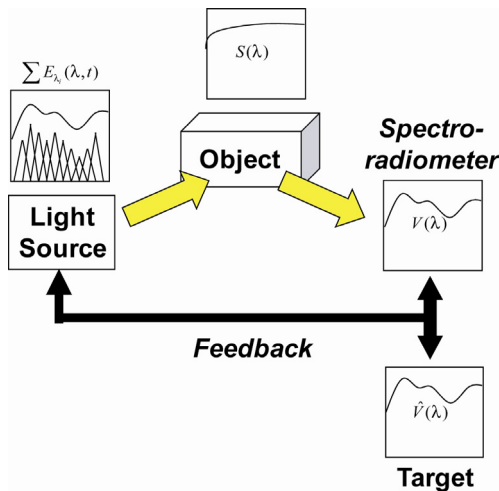
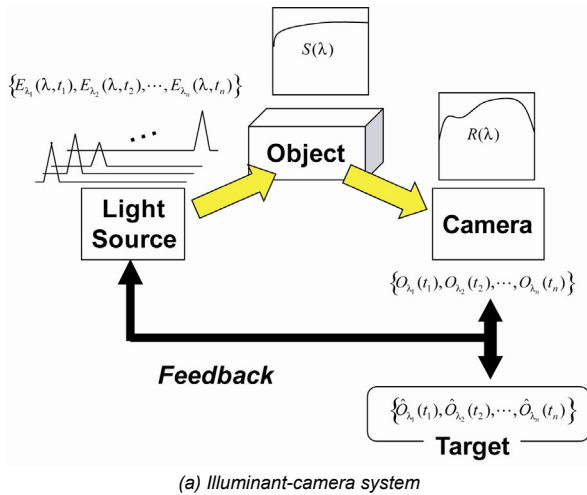


Figure 1 Proposed illuminant control systems.

In our system, we use a monochrome CMOS camera, which has the abilities of 640x480 resolution, 8-bit quantization, and about 200 frames per second (fps). We operate this camera with 320x240 resolution and 10-bit quantization at 20-200fps. Figure 2 shows the spectral-sensitivity function of the monochrome camera. Moreover we investigated a relationship between the input light intensities and the camera outputs. A good linear relationship is obtained at every wavelength.

Basic control of illuminant emission

The light source system can produce emissions at a single wavelength or broad spectrum. We design the emission of a spectral function in two modes of time sequence: steady state and varying with time [3]. In the steady-state mode, the same

spectrum is produced at every time, while in the time-varying mode, different spectra can be produced at every time. Let $E_{\lambda_i}(\lambda)$ be a spectral-power distribution emitted at a central wavelength λ_i . When we consider the time sequence $(E_{\lambda_1}(\lambda), E_{\lambda_2}(\lambda), \dots, E_{\lambda_n}(\lambda))$, the total emission over time produces the spectrum of $E_{\lambda_1}(\lambda) + E_{\lambda_2}(\lambda) + \dots + E_{\lambda_n}(\lambda)$. Figure 3 illustrates an example of spectral-power distributions produced as a time sequence. A set of single spectral functions with narrow width of wavelength is produced at an equal wavelength interval in the visible range. Figure 3 (a) is a 3D perspective view in the time varying mode, where different spectral functions are depicted in time series $E_{\lambda_1}(\lambda, t_1), E_{\lambda_2}(\lambda, t_2), \dots, E_{\lambda_n}(\lambda, t_m)$. Figure 3 (b) is the view in the steady-state mode, where the same spectrum is depicted at every time as $E_{\lambda_1}(\lambda, t) + E_{\lambda_2}(\lambda, t) + \dots + E_{\lambda_n}(\lambda, t)$.

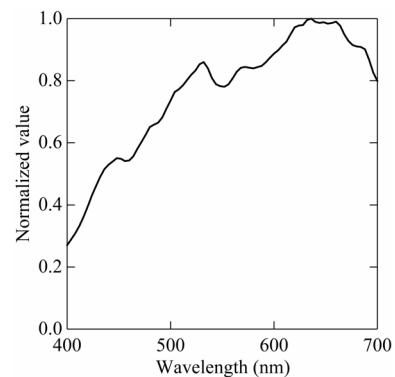


Figure 2 Spectral-sensitivity function of the monochrome camera.

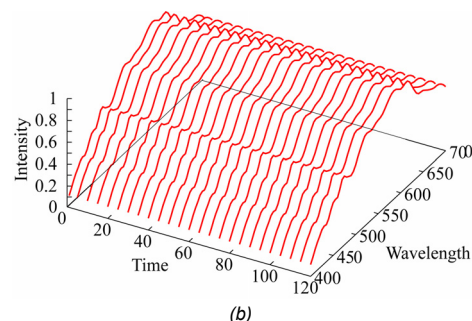
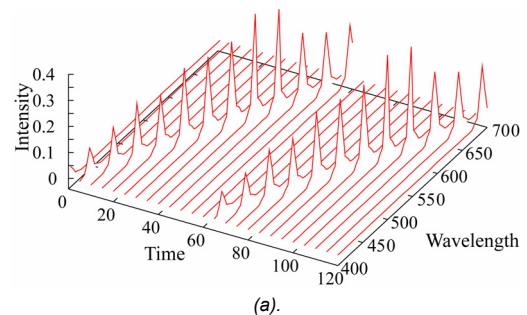


Figure 3 Spectral-power distributions produced as a time sequence. ((a) Time-varying mode, (b) Steady-state mode).

The programmable light source allows creation of our own spectra by changing the properties of wavelength, bandwidth, and relative intensity of multiple basis spectral functions from

imported files. The basis spectra are usually selected from a set of spiky spectra with narrow bandwidth at different wavelengths.

Now we suppose production of the calibrated illuminant of broad spectrum. First, we determine the central wavelength, band width, and relative intensity for each basis spectrum were determined as an initial property. Then, the broad spectrum is produced in the steady state mode based on the imported property file. Figure 4 shows the set of spiky spectra with the bandwidth of 9nm in the equal interval of 10nm. We set the intensity value at every wavelength to the maximum value (100%) in the property file. In Figure 4(a) the solid curves represent the spectra produced at the respective wavelength points, and the broken curve represents the illuminant spectrum directly measured by a spectroradiometer. The synthesized output spectrum is close to the spectral-power distribution of a xenon lamp. These spiky spectra with narrow bandwidth form a set of basis spectra for producing arbitrary illuminant spectra.

Since there is a discrepancy between the produced spectrum in Fig. 4(a) and the target spectrum, we have to adjust the intensity values in the property file for minimizing the discrepancy. For instance, suppose that the target is a constant spectrum. Figure 4(b) shows the produced spectrum after an adjustment. The maximum intensity value is divided by the measurement at each wavelength for the purpose of producing the constant spectrum. However the resulting output spectrum is not always constant as shown in Fig. 4(b). Therefore, additional adjustments are needed. Note that each basis spectrum has a distribution although it is narrow, so that the adjacent spectra overlap on wavelength. Therefore we do not adjust each intensity value independently, but update a set of intensities at a time. The realization by appropriate control becomes the main issue in this study.

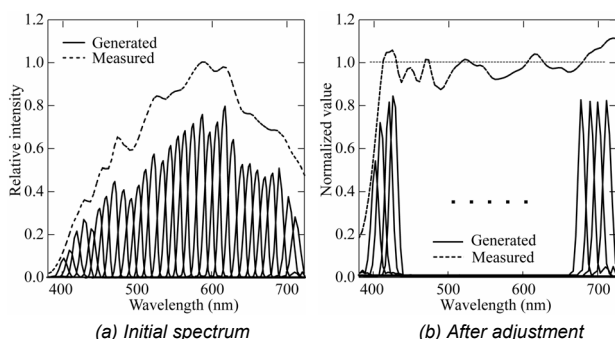


Figure 4 Simple adjustment for obtaining a constant spectral-power distributions.

Feedback Control

Control system

Figure 5 shows the overview of the proposed feedback control system. As mentioned in Fig. 1, we construct two types of systems; illuminant-camera system and illuminant-spectroradiometer system. First we describe the illuminant-camera system in detail. In this system, the light source and the camera are controlled by a personal computer in order to capture image sequences synchronously with the strobe trigger signal. Since the operation of the camera is much slower than the light source, the camera is a master device in the relationship to the light source for their synchronization. In our feedback system, the produced illuminant is irradiated to an object such as a

reference white, and the camera captures the reflected light. Before capturing images, we have to create a sequence of frames forming lighting conditions such as wavelength, bandwidth, and relative intensity [11]. The sequence with appropriate lighting conditions is updated in the feedback process. The detailed algorithm is described in the next subsection. The light source software then prepares a frame by downloading the sequence to RAM and setting the frame up for hardware triggering. When the camera starts observation of a scene, the RS644 strobe signal is output by the instruction from the control PC. The transfer module converts the signal into a TTL signal. The light source follows the TTL falling edge for illuminating next frame of the sequences. Figure 6 summarizes the timing diagram among the control PC, the camera and the light source.

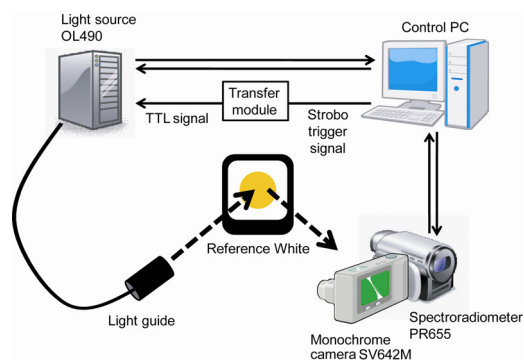


Figure 5 Overview of the feedback control system.

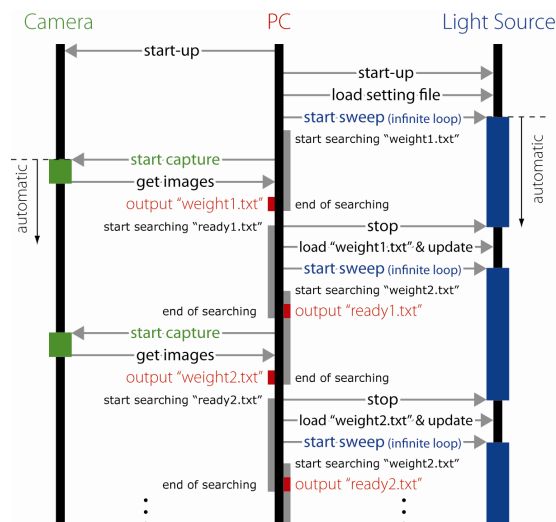


Figure 6 Timing diagram of the proposed control system.

In the case of “illuminant-spectroradiometer” system, the basic construction is the same as the illuminant-camera system. The spectroradiometer (Photo Research, Inc. PR655) becomes the master device in the relationship to the light source for their synchronization.

Control algorithms

Illuminant – camera system

Let $S(\lambda)$ and $R(\lambda)$ be the surface-spectral reflectance function and the sensor-spectral sensitivity function, respectively. When an object surface is illuminated by the light

source with spectrum $E_{\lambda_i}(\lambda, t_j)$, the camera output $O_{\lambda_i}(t_j)$ is described as

$$O_{\lambda_i}(t_j) = \int S(\lambda) E_{\lambda_i}(\lambda, t_j) R(\lambda) d\lambda. \quad (1)$$

For a simple explanation, we assume that the light emitted at a central wavelength λ_i is measured at the time t_j . That is $i=j$. The light source $E_{\lambda_i}(\lambda, t_i)$ is approximated by scaling the intensities of each basis illuminant functions obtained from the xenon lamp as follows:

$$E_{\lambda_i}(\lambda, t_i) \cong \alpha(\lambda_i) L_{\lambda_i}(\lambda, t_i), \quad (2)$$

where $L_{\lambda_i}(\lambda, t_i)$ and $\alpha(\lambda_i)$ are the basis illuminant function and a gain factor at the center wavelength λ_i , respectively. In the active spectral light source, actually, the gain $\alpha(\lambda_i)$ is indicated as the relative intensity in the imported files. Then the optimum estimation of $\{E_{\lambda_i}(\lambda, t_i)\}$ becomes the problem of estimating the optimum gain factor $\{\alpha(\lambda_i)\}$.

For solving this estimation problem, we propose the following iterative algorithm.

(STEP A-1) Determine the target camera output sequence $\{\hat{O}_{\lambda_i}(t_i)\}$.

(STEP A-2) Set initial gain factor as $\alpha(\lambda_i)^{(0)} = 1; \forall i$, and obtain the camera output $O_{\lambda_i}(t_i)^{(0)}$ by illuminating the initial light $E_{\lambda_i}(\lambda, t_i)^{(0)} = L_{\lambda_i}(\lambda, t_i)$ at each time t_i .

(STEP A-3) Update the gain parameter $\alpha(\lambda_i)^{(i)}$; $\forall i$ at iteration time t by

$$\alpha(\lambda_i)^{(i)} = \alpha(\lambda_i)^{(i-1)} \frac{\hat{O}_{\lambda_i}(t_i)}{O_{\lambda_i}(t_i)^{(i-1)}}; \forall i, t \geq 1. \quad (3)$$

The updated $\{E_{\lambda_i}(\lambda, t_i)^{(i)}\}$ is illuminated to the object and the camera output $\{O_{\lambda_i}(t_i)^{(i)}\}$ is obtained again. By increasing the iteration time t , Eq.(2) is estimated iteratively.

According to the relation in Eq.(2), $O_{\lambda_i}(t_i) \propto \alpha(\lambda_i)$. Therefore, it is guaranteed to converge $\hat{O}_{\lambda_i}(t_i)/O_{\lambda_i}(t_i)$ to 1 for each i .

Illuminant – spectroradiometer system

The spectroradiometer observes the spectral distribution $V(\lambda)$ reflected from an object as follows:

$$V(\lambda) = S(\lambda) E(\lambda), \quad (4)$$

Equation (4) is rewritten as

$$V(\lambda, t) = S(\lambda) \sum_i E_{\lambda_i}(\lambda, t) \cong S(\lambda) \sum_i \alpha(\lambda_i, t) L_{\lambda_i}(\lambda, t). \quad (5)$$

For producing a target light source $\hat{E}(\lambda)$, we propose the following iterative algorithm.

(STEP B-1) Determine the target $\hat{V}(\lambda) = S(\lambda) \hat{E}(\lambda)$.

(STEP B-2) Set initial gain factor as $\alpha(\lambda_i, 0) = 1; \forall i$, and measure $V(\lambda, 0)$ by illuminating the initial light $\sum_i E_{\lambda_i}(\lambda, 0) = \sum_i L_{\lambda_i}(\lambda, 0)$.

(STEP B-3) Update the gain parameter $\{\alpha(\lambda_i, t)\}$ at iteration time t by

$$\alpha(\lambda_i, t) = \alpha(\lambda_i, t-1) \frac{\hat{V}(\lambda)}{V(\lambda, t-1)}; \forall i, t \geq 1. \quad (6)$$

The updated $\sum_i E_{\lambda_i}(\lambda, t)$ is illuminated to the object and $V(\lambda, t)$ is measured again. By increasing the time t , Eq.(5) is estimated iteratively.

Note that the estimated spectral distribution $V(\lambda_i)$ is not necessarily proportional to the gain factor $\alpha(\lambda_n)$, because the adjacent basis spectra $L_{\lambda_i}(\lambda)$ and $L_{\lambda_{i+1}}(\lambda)$ are not ideal narrow band so that overlap each other on wavelength λ . Therefore, the convergence of $\hat{V}(\lambda_i)/V(\lambda_i)$ is not guaranteed. However, we can confirm that $\hat{V}(\lambda_i)/V(\lambda_i)$ does not diverge, because $\alpha(\lambda_i)$ is corrected at each n so that the error margin becomes small by Eq.(6).

Applications

Estimation of surface-spectral reflectance by the illuminant-camera system

Illuminant control algorithm

This estimation problem is to recover the surface-spectral reflectance of an object from the camera outputs by using a time-varying mode of active illumination in Fig. 3(a). In Eq.(1), if the light source can be designed as

$$E_{\lambda_i}(\lambda, t_i) = \delta_{\lambda\lambda_i}(t_i) / R(\lambda), \quad (7)$$

then the camera output is written as

$$O_{\lambda_i}(t_i) = S(\lambda) \delta_{\lambda\lambda_i}(t_i) = S(\lambda_i), \quad (8)$$

where δ is the Dirac delta function. Equation (8) shows that the surface-spectral reflectance at the wavelength λ_i is directly obtained from the camera output $O_{\lambda_i}(t_i)$ at each camera pixel. However, the light source cannot produce an ideal delta function. Therefore, even if we know an accurate sensor-spectral sensitivity function $R(\lambda)$, $E_{\lambda_i}(\lambda, t_i) \cong \delta_{\lambda\lambda_i}(t_i) / R(\lambda)$ does not become the best estimate.

In this paper, we do not estimate $E_{\lambda_i}(\lambda, t_i)$ by knowing $R(\lambda)$, but we prepare an object with its surface-spectral reflectance $S(\lambda)$ such as a reference white. We illuminate a set of produced light $\{E_{\lambda_i}(\lambda, t_i)\}$ to the object sequentially, and obtain the camera outputs $\{O_{\lambda_i}(t_i)\}$. Then the light source $\{E_{\lambda_i}(\lambda, t_i)\}$ is updated by iterative processing (STEP A-1) – (STEP A-3) for obtaining the target surface-spectral reflectance. In (STEP A-1), we set the target camera output $\hat{O}_{\lambda_i}(t_i) = c_{\lambda_i}(t_i) S(\lambda_i)$ from the reference object with surface-reflectance $S(\lambda_i)$ at the wavelength λ_i . Where $c_{\lambda_i}(t_i)$ is a normalization factor from the range of the surface-reflectance to the camera output. In our system, we set $c_{\lambda_i}(t_i) = 1023$ because our camera has a 10 bit A/D converter.

The above iterative algorithm generates a sequence of the estimated surface-spectral reflectance ($S(\lambda_1), S(\lambda_2), \dots, S(\lambda_n)$) from the time sequence of the camera outputs ($O_{\lambda_1}(t_1), O_{\lambda_2}(t_2), \dots, O_{\lambda_n}(t_n)$) as

$$S(\lambda_i) = O_{\lambda_i}(t_i) / c_{\lambda_i}(t_i) \quad (i = 1, 2, \dots, n). \quad (9)$$

Experimental result

Figure 7 shows the camera outputs of each iterative stage for producing a spectrum of the reference white object. The spectral curve was produced by combining $n=61$ frames emitted in time series at central wavelengths 400, 405, ..., 700 nm. In this case, we used a reference white plate. The initial sequence of the camera outputs ($O_{\lambda_1}(t_1)^{(0)}, O_{\lambda_2}(t_2)^{(0)}, \dots, O_{\lambda_n}(t_n)^{(0)}$) in Fig. 7(a) was obtained by setting $\alpha(\lambda_n)^{(0)} = 1, \forall n$. By updating the gain parameter $\alpha(\lambda_i)^{(i)}$ using Eq.(3), the camera output was approached to the surface-reflectance of the reference white. Figure 7(d) shows the results at $t=10$.

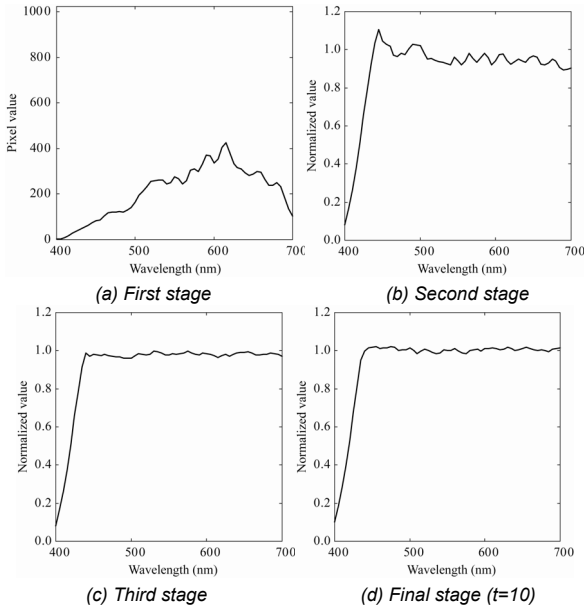


Figure 7 Process for producing a spectrum of reference white on the camera.

It should be noted that we are not free to choose the intensity of the basis illuminant $L_{\lambda}(\lambda)$. If both illuminant intensity and spectral sensitivity are low, the captured image is very dark in the corresponding spectral band, so that the reflectance estimation becomes unreliable. Because of the limitation of maximum illuminant intensity, we determined that the light source takes the maximum intensity in the dark region of 400-435 nm. The constant $c_{\lambda}(t_i)$ in Eq.(9) was derived as $c_{400}(t_1) = 145$, $c_{405}(t_2) = 215$, $c_{410}(t_3) = 310$, $c_{415}(t_4) = 435$, $c_{420}(t_5) = 575$, $c_{425}(t_6) = 720$, $c_{430}(t_7) = 870$, $c_{435}(t_8) = 1010$, $c_{440}(t_9) = \dots = c_{700}(t_{61}) = 1023$.

In order to investigate the produced light source $E_{\lambda}(\lambda, t_i)$, we measure the produced illuminant spectrum which we designed for reflectance estimation in the present system. Figure 8 shows the produced light $E_{\lambda}(\lambda, t_i)$ at time t . Figure 8(a) shows the initial light source by setting $\alpha(\lambda_i)^{(0)} = 1; \forall i$. This spectrum is equivalent to the combination of the basis illuminant function $L_{\lambda}(\lambda, t_i)$. So, the camera output in Fig.7(a) is obtained by illuminating the light in Fig. 8(a). By updating the gain parameter $\{\alpha(\lambda_i)^{(i)}\}$ using Eq.(4), the light source was approached to the inverse function of the camera spectral sensitivity $R(\lambda)$. Figure 8(d) shows the results at $t=10$. In our system, the time for obtaining Fig. 8(d) was around 50 sec.

Figure 9 shows experimental results of surface-spectral reflectance estimation using an X-Rite Mini ColorChecker. The estimated spectral curves of the spectral reflectances are depicted for four patches of red, yellow, magenta and cyan. The broken curves S_m represent the direct measurements by a spectrophotometer, and the solid curves represent the estimation results of $\hat{S} = (S(400), S(405), \dots, S(700))$. Here, S_m and \hat{S} were normalized by the reference white. The numerical error was calculated between the spectral curves of the estimate \hat{S} and the measurement S_m as the RMSE $E = \left(\mathbf{E} \| S_m - \hat{S} \|^2 \right)^{1/2}$. The average RMSE for the 24 color patches in all was 0.020. The estimation time was a few seconds. In Ref.[3], we did the same experiment by adjusting the illuminant manually. The RMSE in Ref.[3] was 0.024 for the same patches. The automatic control system shows a better performance of reflectance estimation, compared with the previous manual adjustment.

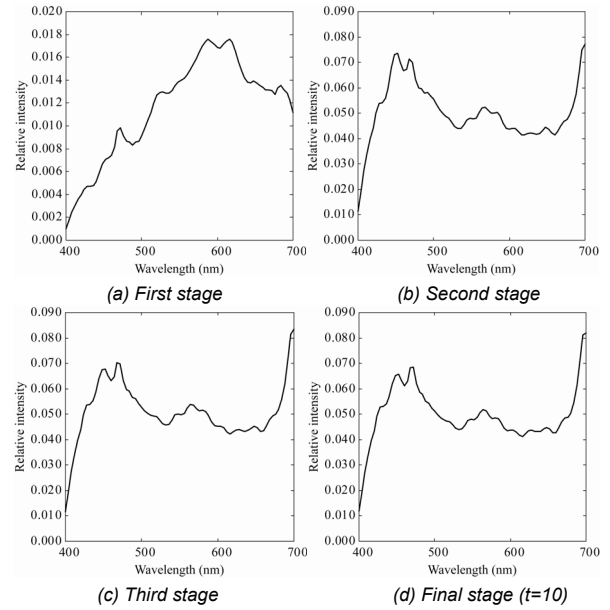


Figure 8 Illuminant spectra produced for obtaining camera outputs in Fig.7. The spectrum is approached to the inverse spectral sensitivity $R(\lambda)$.

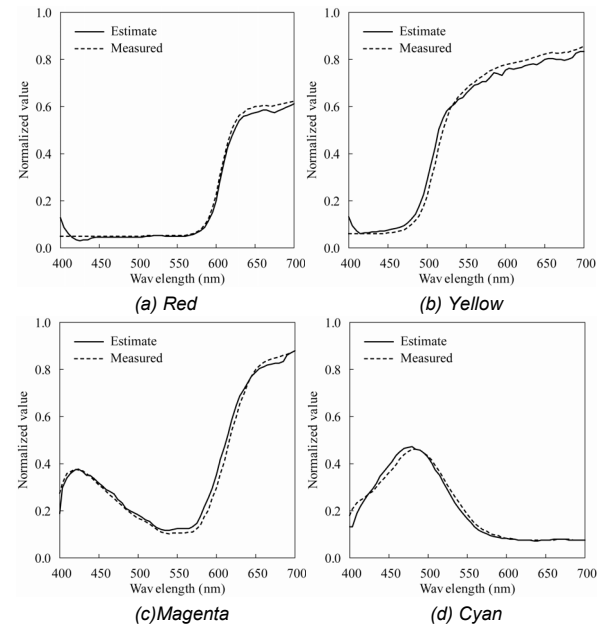


Figure 9 Examples of reflectance estimation results for four patches of a ColorChecker..

Arbitrary illuminant production by the illuminant -spectroradiometer system

We produce an arbitrary illuminant by the proposed illuminant control system. This illuminant is designed using steady-state mode in Fig. 3(b).

The spectral imaging system using an active spectral illumination can provide us an experimental environment to observe object surfaces in a real scene under illuminant with arbitrary spectral-power distribution [3]. Figure 10 shows the convergence process of the illuminant spectral distributions for the target of Illuminant A. We set the intensity value at every wavelength to the maximum value (100%) in the property file. Therefore, Fig. 10(a) is the same as Fig. 4(a). By our feedback

control process as shown in Figs. 10(b)-(d), the produced spectrum was approached to the target spectrum. This suggests a good performance of our system and algorithms. Figure 10 (d) shows the results at $t=10$. It takes about 9 seconds for the control time at each stage. The most time consuming is the process of measuring the reflected light by the spectro-radiometer. Figure 11 shows the RMSE between the target illuminant A and the produced illuminant at each iteration time. The graph shows the good convergence property of the proposed system. Figure 12 shows the result for the illuminant D65. The produced spectrum is almost coincident with the target spectrum.

Conclusions

This paper has proposed an automatic control system for producing arbitrary illuminants on the active spectral light source. Our feedback control system was constructed by combining a high-speed spectral light source and a measurement device such as a high-speed monochrome camera or spectroradiometer. Then we showed feedback algorithms for obtaining the desired illuminant. We demonstrated two applications of the illuminant control system to (1) accurate generation of a target illuminant and (2) estimation of surface-spectral reflectances without knowing the camera spectral sensitivity function.

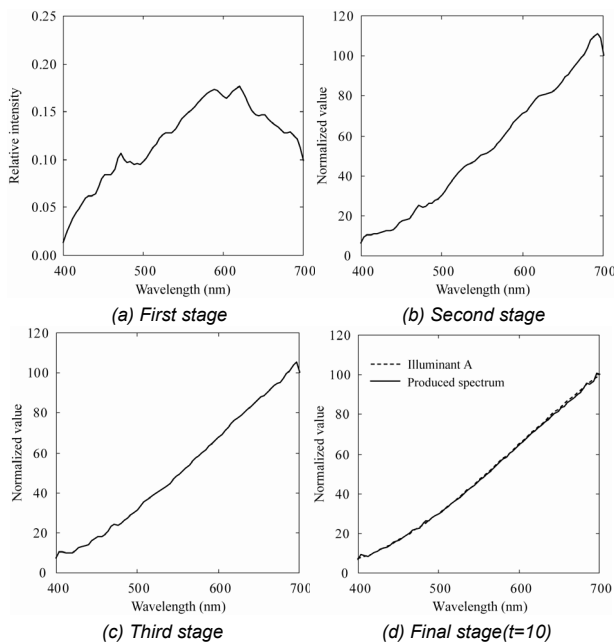


Figure 10 Process for producing illuminant A.

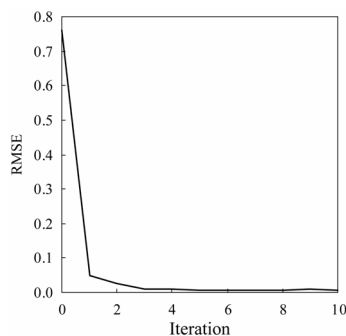


Figure 11 Convergence property of the proposed system.

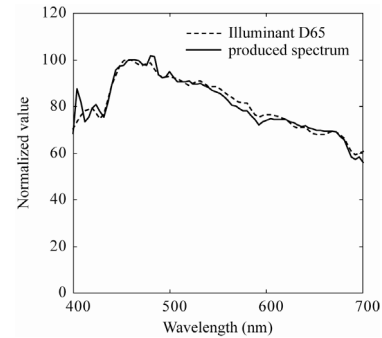


Figure 12 Illuminant spectral distributions produced for Illuminant D65.

References

- [1] Fauch, L., Nippolainen, F., Kamshilin, A., Hauta-Kasari, M., Parkkinen, J. and Jaaskelainen, T., "Optical Implementation of Precise Color Classification Using Computer Controlled Set of Light Emitting Diodes", *Optical Review*, 14(4), 243-245 (2007).
- [2] Part, J.-II, Lee, M.-H., Grossberg, M.D. and Nayar, S.K., "Multispectral Imaging Using Multiplexed Illumination", *Proc. IEEE Int. Conf. Comp. Vis.*, 1-8, Rio de Janeiro, Oct. 2007.
- [3] Tominaga, S., Horiuchi, T., Kakinuma H. and Kimachi, A., "Spectral Imaging with a Programmable Light Source", *Proc. IS&T/SID's 17th CIC*, Albuquerque, Nov. 2009.
- [4] Tominaga, S., Horiuchi, T. and Yoshimura, A., "Real-time color measurement using active illuminant", *Proc. 22nd IS&T/SPIE Symposium on Electronic Imaging*, 7528 San Jose, Jan. 2010.
- [5] Fong, A., Bronson, B. and Wachman, E., "Advanced Photonic Tools for Hyperspectral Imaging in the Life Sciences," *SPIE Newsroom*, (2008).
- [6] Brown, S. W. et al., "Spectrally Tunable Sources for Advanced Radiometric Applications", *J. Res. of the National Institute of standards and Technology*, 111, 401-410 (2006).
- [7] Rice, J. P., Brown, S. W., Neira, J. E. and Bousquet, R. R. "A Hyperspectral Image Projector for Hyperspectral Imagers", *SPIE 6565*, 65650C-1-12 (2007).
- [8] MacKinnon, N., Stange, U., Lane, P., MacAulay C. and Quatrevalet, M., "Spectrally Programmable Light Engine for In Vitro or In Vivo Molecular Imaging and Spectroscopy", *Appl. Opt.*, 44(11), 2033-2040 (2005).
- [9] Chuang, C. H. and Lo, Y. L., "Digital Programmable Light Spectrum Synthesis System using a Digital Micromirror Device", *Appl. Opt.* 45(32), 8308-8314 (2006).
- [10] Hauta-Kasari, M., Miyazawa, K., Toyooka, S. and Parkkinen, J., "Spectral Vision System for Measuring Color Images", *J. Opt. Soc. Am. A*, 16(10), 2352-2362 (1999).
- [11] OL490 Agile Light Source Manual, Optronic Laboratories, (2008).

Author Biography

Takahiko Horiuchi received his B.E., M.E. and Ph.D. degrees from University of Tsukuba in 1990, 1993 and 1995, respectively. He was a member of the Promotion of Science for Japanese Junior Scientists from 1993 to 1995. From 1995 to 1998, he was an Assistant Professor with the Institute of Information Sciences and Electronics, University of Tsukuba. From 1998 to 2003, he was an Associate Professor with the Faculty of Software and Information Sciences, Iwate Prefectural University. In 2003, he moved to Chiba University. He is an Associate Professor at Graduate School of Advanced Integration Science. He is a member of IS&T, IEEE, IEICEJ, CSAJ and IIEEJ.